RESEARCH ARTICLE | JANUARY 15 2019

Advanced small- and wide-angle x-ray scattering beamline for frontier research in biological structures at the Taiwan photon source FREE

Din-Goa Liu ✉; Chien-Hung Chang; Ming-Han Lee; Chin-Yen Liu; Chia-Feng Chang; Liang-Chih Chiang; Ching-Shiang Hwang; Jui-Che Huang; Albert Sheng; Chien-Kuang Kuan; Yi-Qi Yeh; Chun-Jen Su; Kuei-Fen Liao; Wei-Ru Wu; Orion Shih; U-Ser Jeng

AIP Conf. Proc. 2054, 060021 (2019)
https://doi.org/10.1063/1.5084652

Advanced Small- and Wide-angle X-ray Scattering Beamline for Frontier Research in Biological Structures at the Taiwan Photon Source

Din-Goa Liu[1, a)] , Chien-Hung Chang[1], Ming-Han Lee[1], Chin-Yen Liu[1], Chia-Feng Chang[1], Liang-Chih Chiang[1], Ching-Shiang Hwang[1], Jui-Che Huang[1], Albert Sheng[1], Chien-Kuang Kuan[1], Yi-Qi Yeh[1], Chun-Jen Su[1], Kuei-Fen Liao[1], Wei-Ru Wu[1], Orion Shih[1] and U-Ser Jeng[1]

[1]*National Synchrotron Radiation Research Center, 101 Hsin-Ann Road, Hsinchu Science Park, Hsinchu 30076, Taiwan, R.O.C.*

[a)]*Corresponding author: dingoa@nsrrc.org.tw*

Abstract. The TPS 13A biological small-angle X-ray scattering (BioSAXS) beamline under construction is equipped with 4-m IU24 undulator for X-rays in the energy range of E = 4-23 keV (covering the K-edge absorptions from Ca to Ru). The beamline aims for cutting-edge researches in biomacromolecular structures and kinetics, in solid and solution, covering a wide length scale from atomic to micrometer scale and time resolution down to μs. To achieve the goals, the beamline integrates double-multilayer and double-crystal monochromators (DMM/DCM) to have an option of high flux of 4×10^{14} photons/s or a high energy resolution of $\Delta E/E = 1.5\times10^{-4}$. The DCM together with a horizontal four-bounce crystal collimator (4BCC) will be implanted for low beam divergence to perform 2D ultra-SAXS (USAXS). To keep a common X-ray beam path of the operation modes, DMM and DCM are integrated into one rotating cradle in a same chamber for a common beam exit. Microbeam with reasonable beam divergence for SAXS/WAXS structural mapping will be realized with a virtual source defined by a set of high precision/stability slits and another set of K-B mirrors for a focus at the sample position with a demagnification close to 1.3:1. Two beam position monitors, with intensity and position feedbacks respectively to the virtual source slits and the 4BCC and a vertical deflection mirror, are used mainly to stabilize microbeam intensity and position within 1 μm in the vertical and horizontal directions. This TPS 13A BioSAXS beamline will be commissioning at the end of 2019.

INTRODUCTION

During the past few years, increasing more researchers from different institutes have adopted or are interested in biological small-angle X-ray scattering (BioSAXS). The fruitful results with BioSAXS on structural biology have been reported in high impact journals, including Nature, J. Biological Chemistry, and Accounts of Chemical Research [1-3]. Currently, the National Synchrotron Radiation Research Center (NSRRC) also has a joint project with Academia Sinica (under the Taiwan Protein Project) to develop a dedicated, state-of-the-art Bio-SAXS/WAXS beamline with a brilliant undulator X-ray source at the 3 GeV synchrotron Taiwan Photon Source (TPS) of NSRRC. This dedicated TPS BioSAXS beamline is designed to outperform the current TLS SAXS beamline[4-5] to provide opportunities for advanced bio-structural studies. There are four major operation modes with the new beamline, including (1) high flux mode for SAXS/WAXS/UV-Vis with online a high-pressure liquid chromatography (HPLC) instrument for biomacromolecular solution structures and structural kinetics down to microsecond time scale, (2) USAXS mode for resolving hierarchical structures of bio-machinery assembly up to 1-μm length scale, (3) anomalous SAXS (ASAXS) mode for metal or mineral distributions (including Ca atoms) in bio-structures or drug-carriers, and (4) microbeam SAXS/WAXS for structural mapping of natural/synthetic bio-tissues. With these features, the frontier

Proceedings of the 13th International Conference on Synchrotron Radiation Instrumentation – SRI2018
AIP Conf. Proc. 2054, 060021-1–060021-6; https://doi.org/10.1063/1.5084652
Published by AIP Publishing. 978-0-7354-1782-3/$30.00

TPS BioSAXS beamline will cover both the needs of academia research and bio-industrial applications. Below, the design of the TPS BioSAXS beamline is detailed.

PHOTON SOURCE

The BioSAXS beamline located at Port-13A of TPS, of a straight section of 7 m, is equipped with a 4-m in-vacuum undulator (IU24) of 168 magnets arranged in a period length of 24 mm. With the 3.0 GeV electron beam energy of TPS and 500 mA beam current, the 4-m IU24 (of a tunable gap size g between the magnetic poles) provides highly brilliant x-rays in the X-ray energy range of 4 to 23 keV. The energy range is designed to cover the K-edge absorptions from Ca up to Ru. Ca atoms are abundant in biological systems for important functions. The maximum deflection parameter is K (effective) = 1.927 at g = 6.8 mm setting for the first phase of beamline operation; the minimum g value is expected to be 6.0 mm. The X-ray source features of the IU24 of the 13A-BioSAXS beamline are simulated with g = 6.8 mm for optimized performance. The key parameters of the IU24 are listed in Table 1.

TABLE 1. Structural parameters of the IU24 of the TPS 13A beamline

Parameters	Value
Period Length	24 mm
Number of Period	168
Magnetic Peak Field, B_{eff}	0.86 T
Deflection Parameter, K_{eff}	1.927
Total Magnetic Length	4.032 m
Minimum Gap, g	6.8 mm
Photon Beam Size (1σ)@ 4 keV(24 keV)	120(120) μm × 4.3(2.3) μm
Photon Divergence (1σ)@ 4 keV(24 keV)	20(19.4) μrad × 10.3(8.8) μrad

DESIGN OF BEAMLINE OPTICS

The major beamline optical system (Fig. 1) includes integrated double crystal/multilayer monochromators (DCM/DMM), for an option of high energy resolution mode ($\Delta E/E = 1.5\times10^{-4}$) or high flux mode ($\Delta E/E = 1\times10^{-2}$) for time-resolved studies. This is followed by a beam focusing system of the vertical focusing (VFM), horizontal focusing (HFM), and vertical deflection (VDM) mirrors, located respectively at 30 m, 30.6 m and 33 m from the photon source.

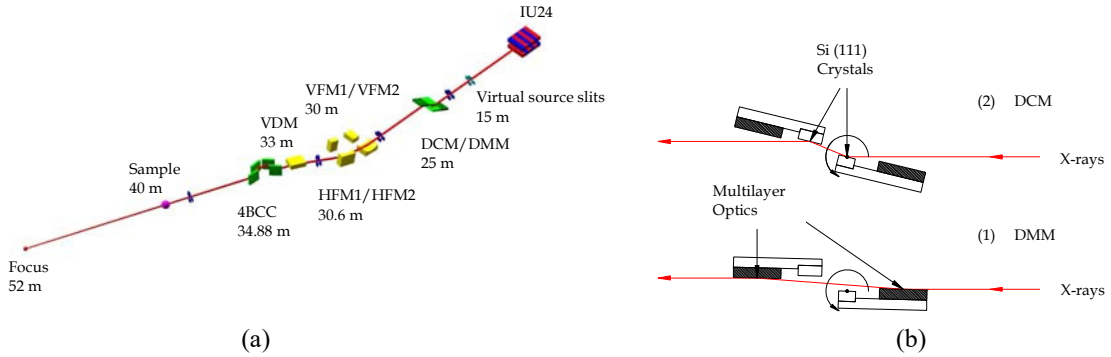

FIGURE 1. (a) The TPS 13A-BioSAXS beamline layout with the IU24 undulator source. The major optical components are as marked, with the corresponding locations indicated. (b) Schematic view of the dual monochromators DCM/DMM, with the rotating center of the whole system situated at the center of the first crystal.

The focus point is set to the end of experimental hutch at ca. 52 m (for a maximum sample-to-detector SD ~ 12 m) to achieve a minimum scattering wavevector q = 0.0003 Å^{-1} (defined by $4\pi\lambda^{-1}\sin\theta$ defined by the X-ray wavelength λ and scattering angle θ). The corresponding resolving characteristic length is up to the order of 1 μm. Following the focusing system is the four-bounce crystal collimator (4BCC) comprising two sets of Si-111 (or Si-331 for optionally

higher collimation) DCM selectively used for an ultra-high collimated beam needed in ultra-SAXS (USAXS) configuration. This is followed by a vertical deflection mirror (VDM) for a leveled beam. For specific beam features requested in different applications, four modes of beam optics sharing a same X-ray path are designed, as detailed below.

(1) High flux mode

In the high flux mode, a flux of ca. 4×10^{14} photon/s at the sample position is planned to perform (1) scanning HPLC/SAXS in millisecond data collection and (2) time-resolved experiments of time resolution down to microseconds with a chopper system. With the data collection time of the order of 1 μs (minimum-resolved time interval) and the scattering efficiency of the typical biomolecule solution, ~5×10^{-4}, we need ~4×10^{14} photon/s to provide ca. 1×10^{5} scattered photons needed in each data frame of 1 μs data collection time. To achieve the high photon flux, double-multilayer monochromator (DMM) with ΔE/E~1% (close to a pink beam mode the IU24), would be used to increase the intensity by a factor of ~10-20, compared to that provided from the Si-111 DCM (ΔE/E~2×10^{-4}). We note that the Mo/B_4C multilayers will be used for the bilayer-based multilayers of DMM (repeat lamellar spacing 25 Å with 200 multilayers and a simulated reflectivity better than 75% when X-ray energy is above 10 keV). The designated optical configuration is shown in Fig. 2; the corresponding spectrum/flux at the sample area with the designed beam optics is shown in Fig. 3

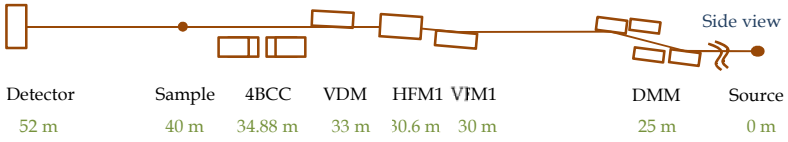

FIGURE 2. A typical layout for the four modes of beamline optics, including the DMM, vertical and horizontal focusing mirrors (VFM and HFM) for a focus point at 52 m from the source, and a vertical deflection mirror (VDM).

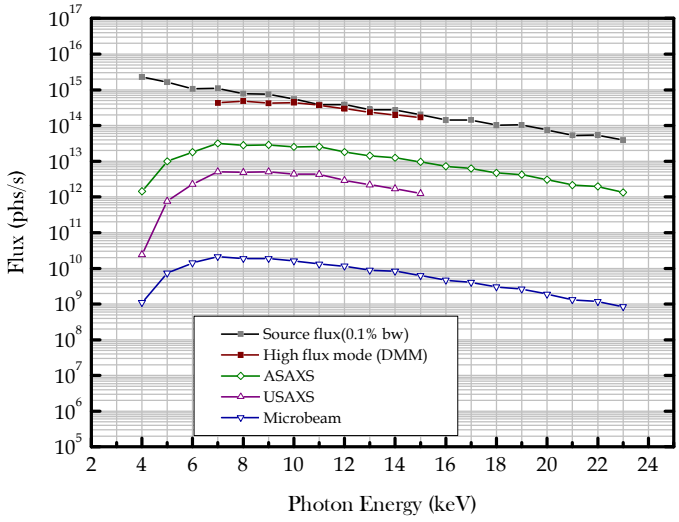

FIGURE 3. Simulated flux spectra at the sample area (40 m from the source) of the IU24 source for the four modes of the optics designs. Note that a microbeam size 7 × 5 μm² is used in the flux calculation.

(2) USAXS mode

In the USAXS mode, the targeted q-minimum measurable is 0.0006 $Å^{-1}$, which is equivalent to a maximum resolvable lamellar spacing of ca. 1 μm (using the Bragg law). For 8.0 keV beam with λ = 1.55 Å, the scattering peak for 1-μm d-spacing separates by 150 μrad from the direct beam, corresponding to 1800 μm at a sample-to-detector (SD) distance of 12 m; with a beamstop of 2-mm dia., the 1-μm scattering peak will be away from the beamstop edge by 800 μm. A collimator of 4BCC (in the horizontal direction) will be used to trim the beam divergence down to ca. 32 × 29 $μrad^2$ (H × V; FW) for a beam size ca. 190 × 36 μm (at the 52 m of the detector position for SD =12 m). To keep the beam size smearing with the 1-μm peak within 1 detector pixel, the horizontal source size will be further trimmed to 1/4 of the source size for a focused beam size (50 × 50 $μm^2$) at the detector to be ca. half of one detector pixel size. A designed USAXS beam optics that can fulfill the requests is illustrated in Fig. 4; which employs the DCM and the same focusing mirrors as the ones used in the high flux mode, added with a four-bounced DCM collimator oriented in the horizontal direction to trim down mainly the horizontal beam divergence.

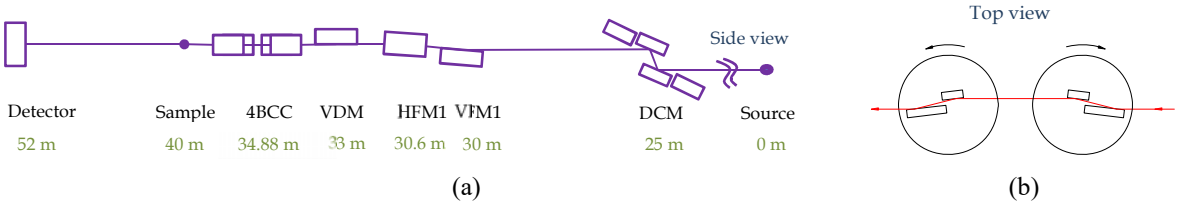

FIGURE 4. (a) Optics design for the USAXS mode. (b) 4-bounce crystal collimator (4BCC) comprising two sets of identical channel-cut Si(111) crystals mounted on synchronized rotary stages with encoder. The beam can bypass the 4BCC when the crystals of the 4BCC is leveled, via the center through channels (6-mm dia.) of the two long crystals.

(3) Anomalous SAXS (ASAXS) mode

The planned TPS BioSAXS beamline provides X-ray flux of ~10^{13} photons/s with the DCM mode in the energy range of 4-23 keV, covering ASAXS for considerable atoms in bio-systems that used in bio-imaging or drug delivery. Especially, ASAXS for Ca ions (K-edge at 4.038 keV) abundant in biological systems can be explored. With the designed DCM energy resolution of $\Delta E/E = 2\times10^{-4}$ for ASAXS measurements with bio-imaging nanoparticles of Gd-silicate:Fe-ITC@$mSiO_2$ or biomarkers of Au NPs, the beam energy can be accurately tuned to (with an energy resolution of a few eV) close to the absorption edges of, for examples, Ca, Gd (L_{III} =7.243 keV) or Au (11.918 keV). The corresponding beam optics design is similar to that used in the high flux mode, except DCM rather than DMM is used for high energy resolution needed in ASAXS. The optics design is shown in Fig. 5.

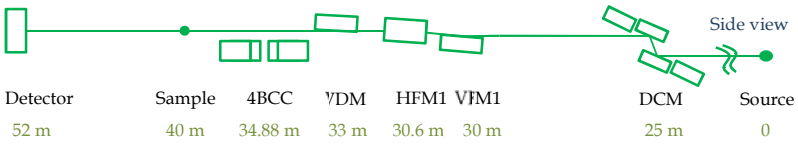

FIGURE 5. Optics design for the ASAXS mode.

(4) Microbeam (μ-beam) SAXS/WAXS mode

With the common parameters of the IU24 source sizes 283 × 7.5 $μm^2$ (FWHM) and source divergence 45 × 21 μrad, a set of high precision, high heat-load slits located at 15.5 m from the IU24 source (in the frontend zone) will be used to regulate the beam size down to 1-10 μm and beam divergence to ca. 15 × 8 $μrad^2$ (FWHM) in H × V directions. The corresponding beam optics design is illustrated in Fig. 6; which optics design includes the DCM, a pair of K-B focusing mirrors (VFM2 and HFM2 that are different from that used in the high flux mode), the same 4BCC, and the same VDM, for a focused beam of dimensions in-between 7 × 5 $μm^2$ at the sample position. With the beam divergence, the beam dimensions broad up to 350 × 50 μm (FWHM) at the detector position at 52 m (i.e. with SD =12 m). Albeit

a low flux calculated, the microbeam optics provides a possibility to perform microbeam USAXS for structural mapping with ~1-μm resolution. To overcome the beam position instability contributed by the thermal vibration of all the optical components, assuming 1 μrad at VDM for 5 μm beam positon fluctuation at the sample positon (at the focus point), sensitive nanometer beam position monitors (NanoBPM) of μm-stability and a feedback (detailed below) will be installed for beam position control (the beamsize at BPM is about 120 μm with the microbeam USAXS optics). The corresponding intensity loss (10^{-7} to 10^{-5}) from the IU24 source is tremendous for a microbeam size of 1 to 10 μm at the sample position; however, this would help to alleviate sample radiation damage issue due to highly focused photon density in the microbeam scanning SAXS/WAXS measurements for structural mapping. The minimum camera length of the SAXS area detector is designed to be 1.0 m from the sample position, covering up to $q \sim 1$ Å^{-1}, with higher X-ray energy of 15 keV; the WAXS area detector aims to cover a q-range between 0.4 to 4 Å^{-1}.

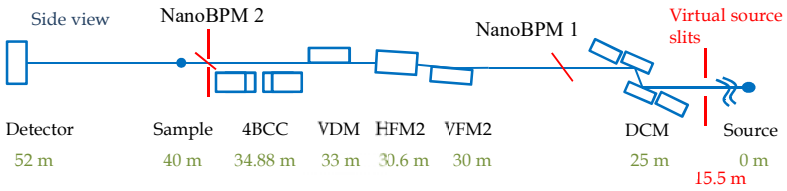

FIGURE 6. Layout for the optics design of the microbeam SAXS/WAXS mode. The beam position monitors NanoBPM 1 and 2 are for feedback controls of the beam intensity and position, respectively .

The beamline performance is summarized in Table 2. The beam sizes, divergences and flux of the several operation modes with a typical 8 keV beam at the sample and detector (52 m for USAXS and 40 m for microbeam) positions. The IU24 source sizes are 283 × 7.5 μm^2 (FWHM) and source divergence 45×21 μrad (FWHM).

TABLE 2. Summary for the performance of different operational modes.

Operational modes	High flux	USAXS	ASAXS	Microbeam
Operation energy range (keV)	7 - 15	4 - 15	4 - 23	7 - 15
Horizontal demagnification	1.36 : 1			1.61 : 1
Vertical demagnification	1.43 : 1			1.45 : 1
Beam size (μm^2)	190 × 52	190 × 36	190 × 36	7 × 5 @ 40 m
Divergence (μrad)	60 × 29	32 × 29	60 × 29	70 × 3.8
Energy resolution	~ 0.2 %	~ 0.02 %		
Flux (phs/s) @ 500mA	~ 4 × 10^{14}	~ 4 × 10^{12}	~ 2 × 10^{13}	~ 1 × 10^{10}

BEAM DIAGNOSTIC AND CONTROL

For a clean fluorescence beam image on the white beam screen 1 (Figure 7) before DCM/DMM when it is moved into the main beam path, the white beam screen is coated with a thin Ni overlayer, to attenuate unwanted visible-light irradiation on the screen from nearby bending magnet sources into the beamline, yet allowing high penetration of the main beam. A set of 10 standard metal foils covering a wide range of K-edge absorption (5-20 keV) is installed shortly after the DCM/DMM for beam energy calibration. A set of slit blades (S2 in Figure 7) positioned shortly behind the DCM and the filter set can read the featured adsorption spectrum via the blade photocurrent induced by the monochrome after a selective foil. With the monochrome beam energy calibrated, alignment of the trajectory of electron beam to the IU24 undulator center line can be done subsequently by optimizing the beam intensity in different harmonic modes at the energy scanned using the DCM. The above design would allow both beam energy calibration with DCM and IU24 alignment at a defined magnet gap. We have estimated the contamination of the higher harmonic X-rays in the X-ray absorption measurements (XAS), taking 7.1 keV beam for an example; the higher harmonic intensity ca. 2.5% should not affect the XAS measurement with an iron foil, in determining the K-edge jump position of Fe.

To monitor the stability of the monochrome beam (especially the microbeam), two on-line beam position monitors with sub-micrometer precision, NanoBPMs, will be installed downstream DCM and VDM for beam diagnostic and

feedback controls (cf. Figure 7). With the beam image reflected by a SiN (1 μm thickness) foil into the CCD of the NanoBPM, the beam center as well as the shape can be tracked in sub-micrometer precision and 20-ms integration time resolution. The first NanoBPM will be used for feedback control of the openings of the high-precision micrometer slits situated at the 15.5 m from the source, for stabilizing the beam intensity; the 2nd set NanoBPM will be used for feedback controls of the positions of the VDM (at 33 m) and the horizontal 4BCC (at 34.88 m) to maintain a beam position stability within 1 μm in both vertical and horizontal directions.

Furthermore, as the beamline covers photon energy below 4 keV, the conventional diamond window for isolating the vacuum environments between the frontend and beamline section and the Be windows between the beamline and endstation sections are replaced by differential pumping designs, respectively, to reduce the intensity loss of low-energy beams.

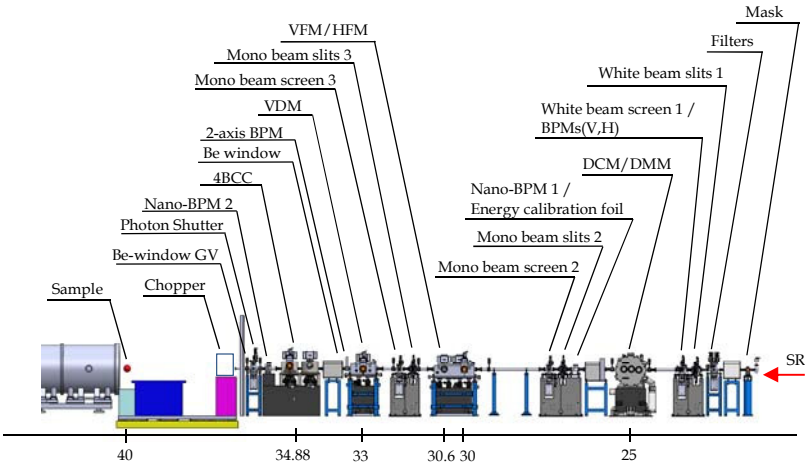

FIGURE 7. Arrangement (numbers are in meter) of the TPS 13A BioSAXS beamline components.

CONCLUSION

The designated TPS BioSAXS beamline provides options with high flux for time-resolved, simultaneous SAXS/WAXS down to 1 μs for biological structures and structural kinetics, microbeam SAXS/WAXS for structural mapping with micrometer resolution, and USAXS with a highly collimated beam for large structural assemblies of ordered length scale up to 1 micrometer. The corresponding designs of the three beam optics share a same X-ray path for easy conversions among the operation modes. This TPS BioSAXS beamline is expected to fulfill the current and future needs of domestic and international researchers on biological structural research.

ACKNOWLEDGMENTS

The authors would like to thank all the staffs at NSRRC who support and help this project.

REFERENCES

1. M. C. Ho, J. F. Menetret, H. Tsuruta and K. N. Aallen, Nature **459**, 393-397 (2009).
2. A. K. Showalter, B. J. Lamarche, M. Bakhtina, M. I. Su, K. H. Tang and M. D. Tsai, Chem. Rev. **106**, 340-360 (2006).
3. K. H. Tang, M. Niebuhr, A. Aulabaugh and M. D. Tsai, Nucleic Acids Res. **36**, 849-860 (2008).
4. D. G. Liu, C. H. Chang, C. Y. Liu, S. H. Chang, Y. F. Song, K. L. Yu, K. F. Liao, P. C. Tseng, C. S. Hwang, C. Y. Huang, L. J. Huang, H. S. Fong, S. C. Chung, M. T. Tang, K. L. Tsang, Y. S. Huang, C. K. Kuan, Y. C. Liu, K. S. Liang, and U. Jeng, J. Synchrotron Rad., **16**, 97–104 (2009).
5. U. Jeng, C. H. Su, C. J. Su, K. F. Liao, W. T. Chuang, Y. H. Lai, J. W. Chang, Y. J. Chen, Y. S. Huang, M. T. Lee, K. L. Yu, J. M. Lin, D. G. Liu, C. F. Chang, C. Y. Liu, C. H. Chang, K. S. Liang, J. Appl. Cryst., **43**, 110-121 (2010).